

FEB 12 1997

# SANDIA REPORT

SAND94-2589 • UC-406 706

Unlimited Release

Printed January 1997

RECEIVED

MAR 05 1997

OSTI

# Optical Diagnostics for Turbulent and Multiphase Flows: Particle Image Velocimetry and Photorefractive Optics

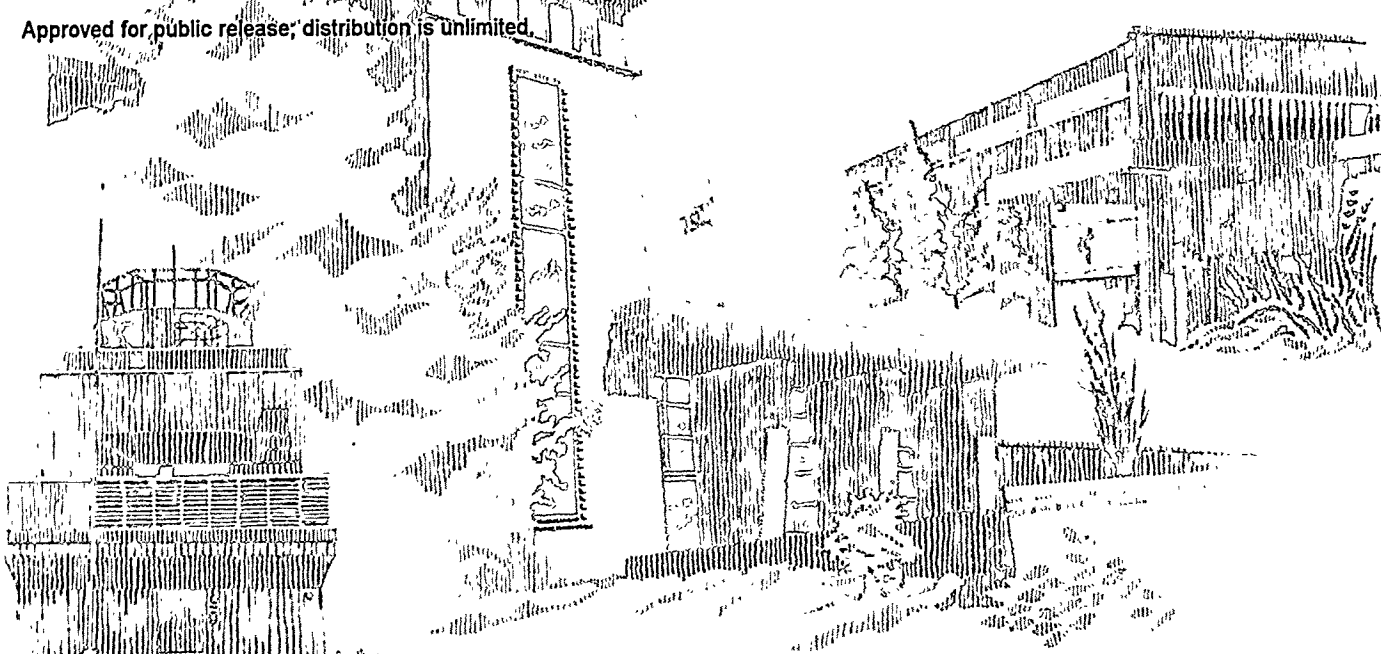
DISTRIBUTION OF THIS DOCUMENT IS UNLIMITED

T.J. O'Hern, J.R. Torczynski, R.N. Shagam, T.K. Blanchat, T.Y. Chu,  
A.L. Tassin-Leger, J.A. Henderson

Prepared by  
Sandia National Laboratories  
Albuquerque, New Mexico 87185 and Livermore, California 94550  
for the United States Department of Energy  
under Contract DE-AC04-94AL85000

MASTER

Approved for public release; distribution is unlimited.



Issued by Sandia National Laboratories, operated for the United States Department of Energy by Sandia Corporation.

**NOTICE:** This report was prepared as an account of work sponsored by an agency of the United States Government. Neither the United States Government nor any agency thereof, nor any of their employees, nor any of their contractors, subcontractors, or their employees, makes any warranty, express or implied, or assumes any legal liability or responsibility for the accuracy, completeness, or usefulness of any information, apparatus, product, or process disclosed, or represents that its use would not infringe privately owned rights. Reference herein to any specific commercial product, process, or service by trade name, trademark, manufacturer, or otherwise, does not necessarily constitute or imply its endorsement, recommendation, or favoring by the United States Government, any agency thereof, or any of their contractors or subcontractors. The views and opinions expressed herein do not necessarily state or reflect those of the United States Government, any agency thereof, or any of their contractors.

Printed in the United States of America. This report has been reproduced directly from the best available copy.

Available to DOE and DOE contractors from  
Office of Scientific and Technical Information  
P.O. Box 62  
Oak Ridge, TN 37831

Prices available from (615) 576-8401, FTS 626-8401

Available to the public from  
National Technical Information Service  
U.S. Department of Commerce  
5285 Port Royal Rd  
Springfield, VA 22161

NTIS price codes  
Printed copy: A05  
Microfiche copy: A01

#### **DISCLAIMER**

**Portions of this document may be illegible  
in electronic image products. Images are  
produced from the best available original  
document.**

## Optical Diagnostics for Turbulent and Multiphase Flows: Particle Image Velocimetry and Photorefractive Optics

T. J. O'Hern, J. R. Torczynski, R. N. Shagam\*, T. K. Blanchat\*\*, T. Y. Chu\*\*,  
A. L. Tassin-Leger, and J. A. Henderson

Engineering Sciences Center

\*Surety Components and Instrumentation Center

\*\*Nuclear Energy Technology Center

Sandia National Laboratories  
P. O. Box 5800  
Albuquerque, New Mexico 87185-0826

### Abstract

This report summarizes the work performed under the Sandia Laboratory Directed Research and Development (LDRD) project "Optical Diagnostics for Turbulent and Multiphase Flows." Advanced optical diagnostics have been investigated and developed for flow field measurements, including capabilities for measurement in turbulent, multiphase, and heated flows. Particle Image Velocimetry (PIV) includes several techniques for measurement of instantaneous flow field velocities and associated turbulence quantities. Nonlinear photorefractive optical materials have been investigated for the possibility of measuring turbulence quantities (turbulent spectrum) more directly.

The two-dimensional PIV techniques developed under this LDRD were shown to work well, and were compared with more traditional laser Doppler velocimetry (LDV). Three-dimensional PIV techniques were developed and tested, but due to several experimental difficulties were not as successful. The photorefractive techniques were tested, and both potential capabilities and possible problem areas were elucidated.

## **Acknowledgment**

This work was supported by the United States Department of Energy under Contract DE-AC04-94AL85000. Sandia is a multiprogram laboratory operated by Sandia Corporation, a Lockheed Martin Company, for the United States Department of Energy. The support of DOE/Sandia Laboratory-Directed Research and Development (LDRD) funds is gratefully acknowledged. The technical assistance of T. W. Grasser in optical configuration, flow facility setup and maintenance, and data acquisition, is greatly appreciated. V. A. Amatucci assisted on the nonlinear optics evaluation.

## Table of Contents

Acknowledgment .....	4
List of Tables .....	7
List of Figures .....	9
Nomenclature .....	13
EXECUTIVE SUMMARY .....	14
<b>1. INTRODUCTION .....</b>	<b>15</b>
<b>1.1 Motivation.....</b>	<b>15</b>
<b>1.2 Program Objectives.....</b>	<b>15</b>
<b>2. PARTICLE IMAGE VELOCIMETRY (PIV) .....</b>	<b>17</b>
<b>2.1 Introduction.....</b>	<b>17</b>
<b>2.2 Two-Dimensional PIV.....</b>	<b>18</b>
<b>2.2.1 Cross-Correlation Algorithm (CCT).....</b>	<b>18</b>
<b>2.2.2 Multi-Frame Tracking Algorithm .....</b>	<b>21</b>
<b>2.3 2D PIV Validation Experiments .....</b>	<b>24</b>
<b>2.3.1 Cavity Flow Experiments .....</b>	<b>24</b>
<b>2.3.1.1 Experimental Setup .....</b>	<b>24</b>
<b>2.3.1.2 Experimental Techniques .....</b>	<b>26</b>
<b>2.3.1.2.1 Laser Doppler Velocimetry (LDV) .....</b>	<b>26</b>
<b>2.3.1.2.2 Particle Image Velocimetry (PIV) .....</b>	<b>27</b>
<b>2.3.1.3 Experimental Approach .....</b>	<b>28</b>
<b>2.3.1.4 Computational Approach .....</b>	<b>29</b>
<b>2.3.1.5 Results of Cavity Flow Study .....</b>	<b>31</b>
<b>2.3.1.5.1 Laser Doppler Velocimetry (LDV) .....</b>	<b>31</b>
<b>2.3.1.5.2 Particle Image Velocimetry (PIV) .....</b>	<b>31</b>
<b>2.3.1.5.3 Computational Simulations (FIDAP) .....</b>	<b>34</b>
<b>2.3.1.5.4 Comparison of Results .....</b>	<b>38</b>
<b>2.3.1.6 Summary and Conclusions .....</b>	<b>39</b>
<b>2.3.2 2D Thermal Convection Experiments .....</b>	<b>40</b>
<b>2.3.2.1 Results .....</b>	<b>45</b>
<b>3. THREE-DIMENSIONAL PARTICLE IMAGE VELOCIMETRY .....</b>	<b>49</b>
<b>3.1 Introduction.....</b>	<b>49</b>
<b>3.2 Three-Dimensional PIV .....</b>	<b>49</b>
<b>3.2.1 Camera Calibration and Particle Combination Theory .....</b>	<b>49</b>
<b>3.2.2 Theory for Tracking Programs .....</b>	<b>55</b>
<b>3.3 3D Validation .....</b>	<b>56</b>
<b>3.3.1 Synthetic Data .....</b>	<b>56</b>
<b>3.3.2 Three-Dimensional Convection Experiment Set-Up .....</b>	<b>57</b>
<b>3.3.3 Results of Three-Dimensional Experiments .....</b>	<b>57</b>
<b>3.4 3D PIV Validation Computations .....</b>	<b>58</b>
<b>4. PHOTOREFRACTIVE OPTICS .....</b>	<b>69</b>
<b>4.1 Introduction.....</b>	<b>69</b>
<b>4.2 Experimental Investigations.....</b>	<b>70</b>

<b>4.3</b>	<b>Experimental Results .....</b>	<b>70</b>
4.3.1	Turbulent Power Spectral Density Measurements .....	70
4.3.2	Temporal Schlieren Visualization.....	71
4.3.3	Orientation Effects on Flow Visualization .....	72
4.3.4	Sensitivity to Wavefront vs. Slope Disturbances .....	73
4.3.5	Effect of Apertures .....	73
4.3.6	Temporal Transmission Measurements .....	73
<b>4.4</b>	<b>Photorefractive PIV .....</b>	<b>74</b>
<b>4.5</b>	<b>Summary .....</b>	<b>74</b>
<b>5.</b>	<b>CONCLUSIONS .....</b>	<b>84</b>
APPENDIX A - PIV Software Operating Manuals .....		85
<b>A. 1.</b>	Instructions for Using PIV Software for 2D Analysis.....	85
<b>A. 2.</b>	Instructions for Using PIV Software for 3D Analysis.....	86
APPENDIX B - 2D and 3D PIV Software: .....		89
REFERENCES.....		97
DISTRIBUTION .....		100

## **List of Tables**

Table 2.2.1. Nondimensionalization of properties.....	59
Table 2.2.2. Nondimensionalization of variables .....	59
Table 2.2.3. Dimensionless parameters .....	59

**This page left intentionally blank**

## List of Figures

<b>Figure 2.1</b> Calculating $C_{ij}$ value for Cross Correlation Tracking (CCT) technique. ....	19
<b>Figure 2.2</b> Intersection of particle images i and j between frames 1 and 2. ....	21
<b>Figure 2.3</b> Determination of possible track for Multiframe Tracking (MFT) technique. ....	22
<b>Figure 2.4</b> Schematic diagram of water channel/cavity flow. ....	25
<b>Figure 2.5</b> Schematic layout of cavity flow system. $D = 3.68$ cm, $L = 3.70$ cm, $h = 1.56$ cm, $w = 7.76$ cm.....	26
<b>Figure 2.6</b> Schematic diagram of computational domain. Channel flow is from lower right to upper left. Symmetry plane (dashed) is exposed to view. ....	29
<b>Figure 2.7</b> Computational meshes (27-node brick elements): top, coarse; bottom, refined. ....	30
<b>Figure 2.8</b> LDV results for cavity flow. Time-averaged centerplane velocity fields. ....	32
<b>Figure 2.9</b> PIV results for cavity flow. Instantaneous centerplane velocity fields. ....	33
<b>Figure 2.10</b> CFD simulations of velocity vectors in the cavity flow at $Re = 600$ . Flow above the cavity is from left to right, with a peak velocity of about 2.8 cm/s. ....	35
<b>Figure 2.11</b> Dimensionless Re-dependence of position ( $X_C, Y_C$ ) of center of main eddy in the symmetry plane $z = 0$ . ....	35
<b>Figure 2.12</b> Streamlines: above, $Re = 3$ (no isolated region); below, $Re = 30$ (isolated region). ....	36
<b>Figure 2.13</b> Topologies: left, low Re; right, high Re. Transition occurs at $Re = 27$ . ....	37
<b>Figure 2.14</b> Comparison of LDV and PIV velocity profiles through the center of primary recirculation region in cavity, for $Re=100$ and $Re=600$ .....	40
<b>Figure 2.15</b> Conceptual representation of a single well of a magma-energy extraction system in operation (cf. Chu et al., 1990). ....	41
<b>Figure 2.16</b> Experimental setup for thermal convection experiments. Dimensions are inches....	42
<b>Figure 2.17</b> Schematic diagram of cooling cylinder inserted into convection tank. ....	43
<b>Figure 2.18</b> 2-D PIV setup for thermal convection experiments. ....	44
<b>Figure 2.19</b> Laser light sheet flow-visualization photographs: (a) slice through cylinder along heater; (b) slice through cylinder across heater. ....	46
<b>Figure 2.20</b> PIV velocity vectors at similar conditions. Left, slice through cylinder along heater strip (plane $x = 0$ ); right, slice through cylinder across heater plane (plane $y = 0$ ). The flow pattern agrees with the flow visualization. Flow is downward beneath cylinder.....	46
<b>Figure 2.21</b> Finite element CFD simulation of selected streamlines in the symmetry planes.....	47
<b>Figure 2.22</b> Streamlines calculated from PIV velocity fields given in Figure 2.20. Qualitative agreement with computational simulation in Figure 2.21 can be seen.....	47
<b>Figure 3.1</b> Three-Dimensional PIV set-up. ....	50

<b>Figure 3.2</b> Simple model of particle determination. ....	55
<b>Figure 3.3</b> Schematic diagrams showing different views of the geometry. ....	61
<b>Figure 3.4</b> Left, coarse mesh. Right, refined mesh. ....	62
<b>Figure 3.5</b> Effect of mesh on $u_z$ and T along $x = y = 0$ (below the cylinder on its axis). ....	62
<b>Figure 3.6</b> Selected streamlines on symmetry planes. ....	63
<b>Figure 3.7</b> Contour plot of $u_x$ ....	63
<b>Figure 3.8</b> Contour plot of $u_y$ . ....	64
<b>Figure 3.9</b> Contour plot of $u_z$ . ....	64
<b>Figure 3.10</b> Contour plot of speed v. ....	65
<b>Figure 3.11</b> Contour plot of pressure p. ....	65
<b>Figure 3.12</b> Contour plot of temperature T. ....	66
<b>Figure 3.13</b> Contour plot of viscosity $\mu$ . ....	66
<b>Figure 3.14</b> Computational results: left, temperature contours; center, velocity vectors; right, selected streamlines on symmetry planes. ....	67
<b>Figure 3.15</b> Laser light sheet flow-visualization photographs: (a) slice through cylinder along heater; (b) slice through cylinder across heater. ....	67
<b>Figure 4.1</b> Schematic layout of optical system for power spectral density (PSD) measurements. Fourier lens 500 mm focal length, relay lens 125 mm focal length. Video camera images Fourier plane of relay lens. ....	75
<b>Figure 4.2</b> Turbulent power spectral density (PSD) measurements. (A) Static background image (no flow). (B) Gas jet: low-flow conditions. (C) Gas jet: high-flow conditions. ....	75
<b>Figure 4.3</b> Schematic layout for photorefractive schlieren technique. Video camera images the phase disturbance plane. ....	76
<b>Figure 4.4</b> Photorefractive schlieren flow visualization with $\text{BaTiO}_3$ . (A) Background field, no flow. (B) $\text{CO}_2$ jet flow field. (C) Jet flow field with background subtracted. ....	76
<b>Figure 4.5</b> Effect of flow perturbation on $\text{BaTiO}_3$ . Test object is hot soldering iron. (A) Static laminar flow. (B) Perturbed flow field (air currents). (C) Perturbed flow field with static flow subtracted. ....	77
<b>Figure 4.6</b> Orientation dependence of a turbulent $\text{CO}_2$ jet in air. (A) Horizontal flow. (B) Vertical flow. (C) Intensity histograms. ....	78
<b>Figure 4.7</b> Dependence of photorefractive effect on gradient orientation. (A, B) Cross flow. (C, D) With flow. Crystal fanning is in vertical direction. ....	79
<b>Figure 4.8</b> Schematic of phase sensitivity test setup. ....	79
<b>Figure 4.9</b> Phase shift test. ....	80

<b>Figure 4.10</b> Effect of cross-coupling beams within crystal. The arrows point to regions of temporally modulated fringes. ....	80
<b>Figure 4.11</b> Effect of a vertical aperture on wavefront extinction: fanning direction vertical. ...	81
<b>Figure 4.12</b> Effect of a horizontal aperture on wavefront extinction: fanning direction vertical.	81
<b>Figure 4.13</b> Crystal extinction vs. time for a variety of initial poling (erasure exposure) times. Incident laser power constant. ....	82
<b>Figure 4.14</b> Crystal peak transmission vs. poling time. ....	83
<b>Figure A.1</b> Basic outline for PIV software for 2D and 3D analysis .....	88

**This page left intentionally blank**

## Nomenclature

$C_{ij}$	Correlation coefficient - used in cross-correlation tracking technique
CCT	Cross-Correlation Tracking
$D_{ij}$	Amount that the diameters of overlapping particles i and j - used in cross-correlation tracking technique
MFT	Multi-Frame Tracking algorithm
$N_{ij}$	Number of particles that overlap between Images i and j - used in cross-correlation tracking technique
$R_{ij}$	pair reliability index - used in cross-correlation tracking technique
$R_n$	Radius of search circle - used in multi-frame tracking technique
Re	Reynolds number for cavity flow = $\bar{u}(2h)/v$
D	Cavity Depth = 3.68 cm (Figure 2.5)
L	Cavity Length in Streamwise direction = 3.70 cm (Figure 2.5)
h	channel depth upstream of cavity = 1.56 cm (Figure 2.5)
w	channel/cavity cross-stream width = 7.76 cm (Figure 2.5)
$u_x$	velocity component in the x direction
$u_y$	velocity component in the y direction
$u_z$	velocity component in the z direction
$u_{av}$	channel mass-flow velocity
$X_C$	X center of main eddy in cavity flow (Figure 2.11)
$Y_C$	Y center of main eddy in cavity flow (Figure 2.11)
$\sigma_l$	Standard deviation from the mean for the lengths of the vectors
$\sigma_\theta$	Standard deviation from the mean for the angles in the x-y plane
$\sigma_\Phi$	Standard deviation from the mean for the angles from the z axis
$\sigma$	Total standard deviation
$L_{x-y}$	Length between particles between frames x and y
$\theta_{1-3}$	Angle in the x-y plane between $l_{1-2}$ and $l_{2-3}$
$\theta_{2-4}$	Angle in the x-y plane between $l_{2-3}$ and $l_{3-4}$
$\Phi_{1-3}$	Angle from the z axis between $l_{1-2}$ and $l_{2-3}$
$\Phi_{2-4}$	Angle from the z axis between $l_{2-3}$ and $l_{3-4}$
$\bar{L}$	Average displacement of particles between frames = $(L_{1-2} + L_{2-3} + L_{3-4})/3$
$\bar{\theta}$	Average $\theta$ of the track = $(\theta_{1-3} + \theta_{2-4})/2$
$\bar{\Phi}$	Average $\Phi$ of the track = $(\Phi_{1-3} + \Phi_{2-4})/2$

## **Executive Summary**

This report summarizes the work performed under the Sandia Laboratory Directed Research and Development (LDRD) project “Optical Diagnostics for Turbulent and Multiphase Flows.”

Advanced optical diagnostics have been investigated and developed for flow field measurements, including capabilities for measurement in turbulent, multiphase, and heated flows. Particle Image Velocimetry (PIV) includes several techniques for measurement of instantaneous flow field velocities and associated turbulence quantities. Nonlinear photorefractive optical materials have been investigated for the possibility of measuring turbulence quantities (turbulent spectrum) more directly.

The two-dimensional PIV techniques developed under this LDRD were demonstrated to work well and were compared with more traditional laser Doppler velocimetry (LDV), and with computational simulations. Two-dimensional benchmarking experiments included flow in a driven cavity and natural convection in a simulated magma chamber. Three-dimensional PIV techniques were developed and tested on the thermal convection experiment but were unsuccessful due to several experimental difficulties.

The nonlinear photorefractive crystal BaTiO<sub>3</sub> has been demonstrated as a significant visualizer of turbulent vs. steady-state flow. However, we have identified two potentially significant limitations in that it (1) appears to visualize gradients differently, depending upon the relative orientation of the gradient to the crystal fanning orientation, and (2) visualizes refractive gradients, not absolute phase change, as previously reported in the literature. The desired quantification of photorefractive measurements proved to be very difficult for these reasons.